

The Smoking Guns Of Neutron Stars Mergers

S. DADO⁽¹⁾, A. DAR⁽¹⁾

⁽¹⁾ *Department of Physics, Technion Israel Institute of Technology, Haifa 32000, Israel*

Summary. —

The short hard gamma ray burst (SHB) 170817A that followed the first neutron stars merger (NSM) detected in gravitational waves (GWs) has shown beyond doubt that NSMs produce SHBs. Its low luminosity and other properties that differ from those of ordinary SHBs, were predicted by the cannonball model of GRBs for relatively nearby SHBs, which almost entirely are low luminosity SHBs viewed from far off-axis. Such far off-axis low luminosity SHBs are mostly the smoking guns of only nearby NSMs, like those detectable by Ligo-Virgo. The smoking guns of much more distant NSMs are PWN afterglows powered by the spin-down of the nascent n*s, preceded by a visible SHB, or by an invisible SHB, which is beamed away from Earth.

1. – Long history in short

Gamma ray bursts were discovered in 1967 by the U.S. Vela spy satellites (Klebesadel, Strong & Olson 1973). They seem to be divided into two distinct classes, long duration gamma ray bursts (GRBs) that usually last more than 2 seconds and short hard bursts (SHBs) that usually last less than 2 seconds (Norris et al. 1984; Koveliotou et al. 1993). While there is clear observational evidence for production of long duration GRBs in broad line supernova explosions (SNe) of type Ic (e.g., Galama et al. 1998; Dado, Dar & De Rujula (hereafter DDD) 2002; Stanek et al. 2003; Hjorth et al. 2003; Zeh et al. 2004; and references therein), and perhaps in phase transition of neutron stars (SN-less GRBs) in high mass X-ray binaries (Dado & Dar 2018), until August 17, 2017 neither the origin nor the production mechanism of SHBs were established observationally (see, e.g. Berger et al. 2013; Berger 2014 for a review).

The year 1967 was also the discovery year of the first pulsar by Jocelyn Bell and Antony Hewish (1967). Shortly later, Franco Pacini (1967) suggested that pulsars are fast spinning neutron stars with a large magnetic field whose existence was suggested by Walter Baade and Fritz Zwicky (1934). Eight years later, Russel Hulse and Joseph Taylor (1975) published their discovery of the first binary pulsar PSR B1913+16, which led Wagoner (1975) to suggest timing measurements of PSR B1913+16 for testing the

existence of gravitational radiation predicted by general relativity. Follow-up timing observations by Taylor and Weisberg (1984,1989) of the spiral-in of the pulsars in PSR B1913+16 confirmed the behavior predicted by General Relativity.

The evidence on spiral-in of the n*s in PSR B1913+16 led Goodman, Dar and Nussinov (1987) to suggest that GRBs may be produced in external galaxies by neutrino-antineutrino annihilation $e^+e^-\gamma$ fireballs (Goodman 1986) around the nascent compact object -a massive neutron star, quark star, or black hole- not only in stripped envelope supernova explosions, but also in mergers of neutron stars (n*s) in compact n*n* binaries.

However, observations with the Compton Gamma-Ray Burst Observatory (CGRO) shortly after its launch in 1991 indicated that GRBs are extragalactic and mostly at very large cosmological distances (Meegan et al. 1992) such that neutrino-annihilation fireballs around nascent neutron stars and black holes in stripped envelope supernovae and merger of neutron stars, are not powerful enough to produce observable GRBs. Consequently, Shaviv and Dar (1995) suggested that GRBs are produced by narrowly collimated jets of highly relativistic plasmoids (cannonballs) of ordinary matter by inverse Compton scattering (ICS) of light surrounding their launch sites. Such jets can be launched in merger of compact stars (Goodman, Dar and Nussinov 1987) due to the emission of gravitational waves, in a phase transition of neutron stars to a more compact object (quark star or black hole) following mass accretion in compact binaries, or in stripped-envelope core-collapse supernova explosions (Goodman, Dar and Nussinov 1987, Dar et al. 1992).

The localization of GRBs with BeppoSAX (Costa et al. 1997) led to the discovery of the GRB afterglow at longer wave lengths, which led to the discoveries of their host galaxies, their redshifts, the SN-GRB association, SN-less GRBs, and the detailed properties of their prompt and afterglow emissions over the entire electromagnetic spectrum. These achievements were mainly due to space based observatories such as BeppoSAX, HETE, Swift, Konus-Wind, Fermi, CXO, and XMM-Newton, Hubble Space Telescope, and to many ground based telescopes, during the past two decades.

The mounting data on GRBs, SHBs, their afterglows and their environments from these observations in the past two decades have been analyzed mainly with two theoretical models, the fireball model (e.g., Piran 1999; Meszaros 2001; and references therein) and the cannonball model (e.g., Dar & De Rujula 2004 and references therein). Both models were claimed to reproduce well these data. But critical tests of the key falsifiable predictions of these models (e.g., Dado & Dar 2016 and references therein), which did not involve free adjustable parameters and multiple choices, have clearly indicated that the fireball model is neither a reliable physical model of GRBs nor of SHBs despite its wide use and misleading claims of success. These are in contrast to the cannonball model, which reproduces well the measured lightcurves of GRBs and SHBs and its falsifiable predictions have been repeatedly demonstrated to be well satisfied by the observational data on GRBs and SHBs (Dado & Dar to be published).

GW170817, the first NSM event detected in gravitational waves on August 17, 2017 by Ligo-Virgo (Abbott et al. 2017a,b,c), was followed by a short gamma ray burst, SHB170817A, detected by the Fermi (von Kienlin et al. 2017) and Integral (Savchenko et al. 2017) satellites. It began 1.74 ± 0.05 s after the chirp ending the arrival of gravitational waves from GW170817. It was the first indisputable NSM-SHB association, indicating that SHBs probably are the smoking guns of neutron star mergers, despite the fact that SHB170817A and its afterglow appeared very different from all SHBs and SHB afterglows observed before. The different observed properties of SHBs following NSM detections by the current Ligo-Virgo detectors, were predicted by Dado and Dar (2017) two days before

the GW170817-SHB170817A event. In the CB model, SHBs are highly beamed. Because of that and the small rate of NSM events within the detection horizon of Ligo-Virgo, such NSMs produce mainly far off-axis SHBs, which appear different from very distant SHBs, most of which are observed from near axis.

2. – The prompt emission

In the CB model, the gamma-ray generating mechanism in SHBs is ICS of a light (glory) surrounding the launch site of a highly relativistic jet of CBs launched by fall-back ejecta on the nascent compact object (neutron star, quark star, or a stellar black hole) Macias in NSMs.

The delay of ~ 1.74 s in the arrival time of the first γ -rays of SHB170817A after the chirp ending the arrival of gravitational waves from GW170817 may be due to the fall back time of ejecta from the NSM.

The glory around binary pulsars. Young pulsars are usually surrounded by a pulsar wind nebula (PWN) (Weiler & Panagia 1978; for a review, see, e.g., Gaensler & Slane 2006), which absorbs the magnetic dipole radiation, relativistic wind, high energy particles and ejecta emitted from the pulsars, and converts their energy to a glory with an exponentially cutoff power-law spectrum with a peak energy flux around 1 eV (see, e.g., Macias-Perez et al. 2010; Tanaka & Takahara 2010 and references therein). The observed duration of the SHB pulses in SHBs requires a glory of a typical size $R \sim 10^{15}$ cm. Such a relatively small size PWN may be quite natural for very compact neutron stars (n^* s) binaries. Assuming that both n^* s may be approximated by point masses in a circular orbit, their separation a decreases at a rate $da/dt = -a/t_{GW}$, where the merger timescale due to the gravitational radiation is given in geometrized units ($G=c=1$) by $t_{GW} = (5/64)a^4/\mu M^2$. $M = M_1 + M_2$ is the total mass and $\mu = M_1 M_2 / (M_1 + M_2)$ is the reduced mass of the n^*n^* binary. For canonical neutron stars, with $M_1 = M_2 = 1.4M_\odot$ and initial separation a , the merger time due to gravitational radiation is $t_m = \int (dt/da) da \approx 1.76 (a/2R_\odot)^4$ Gy. This suggests that n^*n^* binaries with a merger time much shorter than the Hubble time must be born in very compact binaries where $a \ll R_\odot$. Such compact binaries may be formed either in a single SN explosion of a massive star by fission of its fast rotating core during its rapid collapse, or, perhaps, in two separate SN explosions in massive star binaries where dynamical friction in a common envelope phase shrinks the binary separation (e.g., Bhattacharya & van den Heuvel 1991; Lorimer 2008 and references therein).

The $E_p - E_{iso}$ correlation and SHB170817A. The CB model entails very simple correlations between the main observables of SHBs, and of GRBs (Dar & De Rujula 2000a). For instance, a burst at redshift z and Doppler factor $\delta \simeq 2\gamma/(1+\gamma^2\theta^2)$, the peak energy of their time-integrated energy spectrum satisfies $(1+z)E_p \propto \gamma\delta$, while their isotropic-equivalent total gamma-ray energy is $E_{iso} \propto \gamma\delta^3$. Consequently, in ordinary GRBs and SHBs, mostly viewed from an angle $\theta \approx 1/\gamma$,

$$(1) \quad (1+z)E_p \propto [E_{iso}]^{1/2},$$

while in far off-axis ($\theta^2 \gg 1/\gamma^2$) ones,

$$(2) \quad (1+z)E_p \propto [E_{iso}]^{1/3}.$$

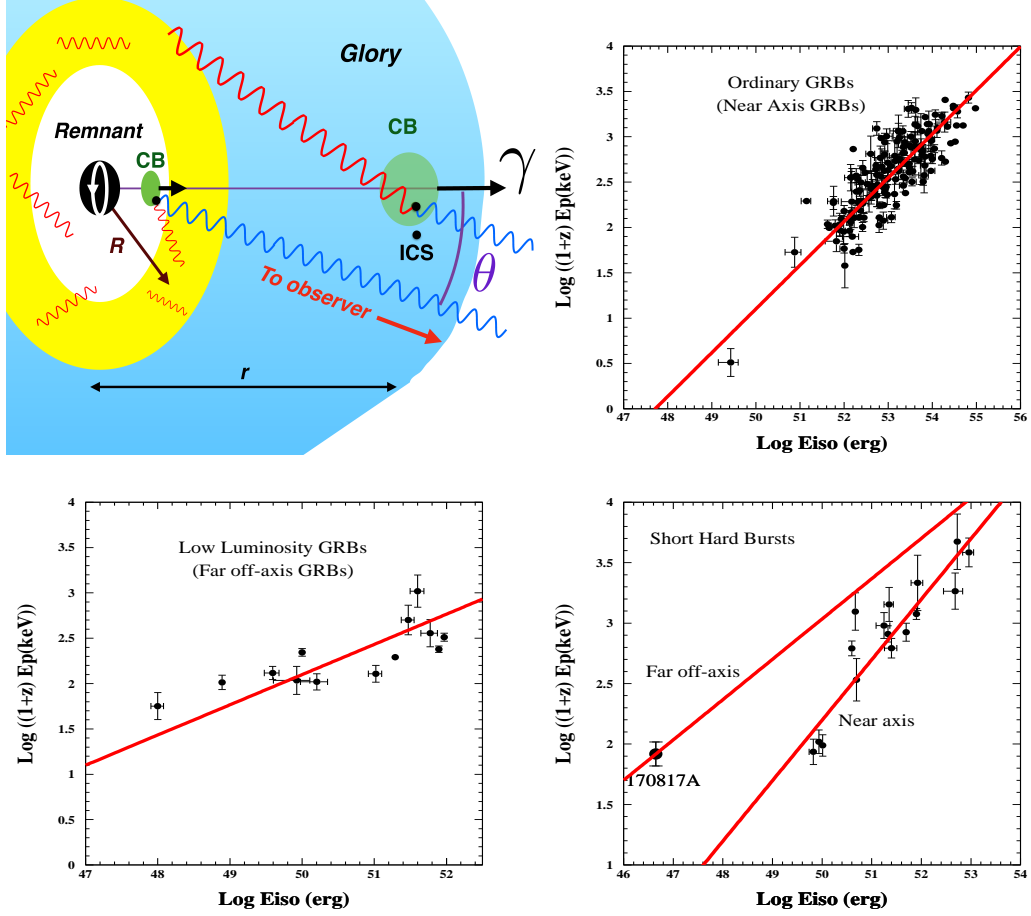


Fig. 1. – Upper left: A CB as it crosses and exits the blue glory of a yellow toroidal PWN around NSM. The CB’s electrons Compton up-scatter glory photons with incident angles which decrease with increasing distance from the CB launch point. Upper right: The $[E_p, E_{\text{iso}}]$ correlation for near axis GRBs. Bottom: The $[E_p, E_{\text{iso}}]$ correlation for far off-axis GRBs (left) and SHBs (right). The lines are the CB model predictions, Eqs.(1),(2), for near and far off axis cases.

The correlations summarized in Eq.(1) for near axis GRBs, later discovered empirically by Amati et al. (2002), and for near axis SHBs, are shown in Figure 1. Also shown there is the correlations represented by Eq.(2) for far off-axis GRBs and SHBs. As shown, both near axis GRBs and SHBs, and far off-axis GRBs satisfy well the predicted correlations. Eq.(2) for low luminosity (far off-axis) SHBs, however, cannot be tested yet because of lacking data on low luminosity SHBs.

The far off-axis viewing angle of SHB170817A. In the CB model, the relatively small $E_{\text{iso}} \approx 5.4 \times 10^{46}$ erg (Goldstein et al. 2017) of SHB170817A suggests that it is viewed far off-axis. This is supported by its relatively large E_p as can be seen from Figure 1. Far off-axis viewing angles yield $\gamma \delta \approx 2/\theta^2$. Hence, ICS of a glory with a peak photon energy $\epsilon_p \approx 1$ eV by a jet, which is viewed from far off-axis, yields $(1+z)E_p \approx 2\theta^2$ eV. The T_{90} measured $E_p = 82 \pm 23$ keV of SHB170817A (von Kienlin et al. 2017) yields

a viewing angle $\theta \approx \sqrt{2/82 \times 10^3} \approx 5 \times 10^{-3}$. Such a small viewing angle appears to imply a very small probability of NSM170817 to produce an SHB visible from Earth. However, neither the number of CBs launched in an NSM, nor their time sequence, nor their emission directions, are predicted by the CB model. A shotgun configuration of the emitted CBs, and/or a precession of the emission direction, as observed in pulsars and microquasars, combined with relativistic beaming, can make only a small fraction of the emitted CBs visible. That, and the very near locations of SHB170817A can enhance the detection rate of such events by a large factor compared to that estimated from the assumption that only the CBs which produced the observed light curves were actually emitted.

More information from E_p and E_{iso} . The canonical value $\gamma \approx 1000$ deduced for ordinary SHBs (e.g., DDD 2009b), and a viewing angle $\theta \approx 5$ mrad, yield $\delta = 80$. In the Thomson regime ($2\gamma\epsilon \ll m_e c^2$), the distribution of the incident photons after Compton scattering in the CB is nearly isotropic. In the observer frame this distribution becomes $dN_\gamma/d\Omega = N_\gamma \delta^2/4\pi$. Hence, the canonical $\gamma \approx 1000$ of CBs extracted from ordinary SHBs (e.g., Dado et al. 2009b), $E_{iso} \approx 5.4 \times 10^{46}$ erg (Goldstein et al. 2017), and $E_p = 82$ keV (von Kienlin et al. 2017) in SHB170817A, yield a total number of ICS photons $N_\gamma = E_{iso}/E_p \delta^2 \approx 6.4 \times 10^{49}$, and a total γ -ray energy $E_\gamma \approx \epsilon_p \gamma^2 N_\gamma \approx 1.0 \times 10^{44}$ erg.

Assuming that ejected CBs in NSMs are made of n^* surface material, i.e., mainly iron nuclei with roughly equal number of protons and neutrons (Chamel & Haensel 2008, and references therein), and that the kinetic energy of the CB electrons powers the prompt γ -ray emission by ICS of glory light, then, in the CB model, the estimated kinetic energy of the CB in SHB170817A was $E_k \approx 2 m_p E_\gamma/m_e \approx 3.7 \times 10^{47}$ erg, and its baryon number was $N_b \approx E_k/m_p c^2 \gamma \approx 2.5 \times 10^{47}$.

In the CB model, the peak time Δ of the prompt emission pulse is reached when the CB becomes transparent to photons, i.e., when the photon's mean diffusion time t_d out of the CB satisfies $R_{CB}^2/(c\lambda) = \Delta$. The photon's mean free path λ that is dominated by Thomson scattering on free electrons is given by $\lambda = 4\pi R_{CB}^3/(N_e \sigma_T)$ where $\sigma_T = 0.67 \times 10^{-24} \text{ cm}^2$ is Thomson cross section, and the electron number of the CB satisfies $N_e \approx N_b/2$. Thus, the peak time of the ICS pulse in SHB170817A formed by CB with $N_e \approx N_b/2 \approx 1.25 \times 10^{47}$, which is expanding with a speed of sound in a relativistic gas, $v = c/\sqrt{3}$, is expected to occur at $\Delta \approx 3\sqrt{3} N_e \sigma_T / 4\pi c^2 \delta = 0.69$ s.

The mean photon density n_g of the glory in the volume V where from the SHB photons were scattered, satisfies $N_\gamma = n_g V \approx n_g \pi \gamma \delta^3 c^3 \Delta^3/9$. It yields $n_g \approx 4.0 \times 10^{10} \text{ cm}^{-3}$ for a peak time $\Delta \approx 0.69$ s of the prompt emission pulse of SHB170817A.

The pulse shape. The observed pulse-shape produced by IC of glory light with an exponentially cut off power law (CPL) spectrum, $dn_g/d\epsilon \propto \epsilon^{-\alpha} \exp(-\epsilon/\epsilon_p)$ at redshift z , by a CB is given approximately (see, e.g., Eq. (12) in DDD 2009b) by

$$(3) \quad E \frac{d^2 N_\gamma}{dE dt} \propto \frac{t^2}{(t^2 + \Delta^2)^2} E^{1-\alpha} \exp(-E/E_p(t))$$

where Δ is approximately the peak time of the pulse in the observer frame, which occurs when the CB becomes transparent to its internal radiation, and $E_p \approx E_p(t = \Delta)$.

In Eq.(3), the early temporal rise like t^2 is produced by the increasing cross section, $\pi R_{CB}^2 \propto t^2$, of the fast expanding CB when it is still opaque to radiation. When the CB becomes transparent to radiation due to its fast expansion, its cross sections for ICS becomes $\sigma_T N_e! \approx \text{const.}$ That, and the density of the ambient photons, which for

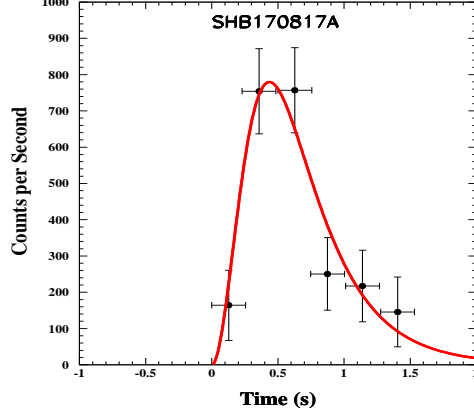


Fig. 2. – Comparison of the pulse shape for $E_m = 50$ keV of the first pulse of SHB170817A measured by Goldstein et al. (2017) and the CB model pulse shape as given by Eq.(3).

a distance $r = \gamma \delta c t / (1+z) > R$ decreases like $n_g(r) \approx n_g(0) (R/r)^2 \propto t^{-2}$, produce the temporal decline like t^{-2} .

The ICS of glory photons with energy ϵ by the CB electrons boosts their energies to observed energies $E = \gamma \delta (1 + \beta \cos \theta) \epsilon / (1+z)$. The unknown geometry of the PWN of n*n* binaries can be very complex and different in different SHBs. The glory, however, may attain a more universal shape, in particular outside the PWNs. To demonstrate the effect of the increasing anisotropy of the glory photons when a CB moves away from its launch point, consider for simplicity a CB launched along the axis of a glory of torus-like PWN with a radius R , as illustrated in Figure 1. In that case $\cos \theta = -r / \sqrt{r^2 + R^2}$ for glory photons which intercept the CB at a distance r from the center. It yields a t -dependent

$$(4) \quad E_p(t) = E_p(0) [1 - t / \sqrt{t^2 + \tau^2}]$$

with $\tau = R(1+z) / \gamma \delta c$ and $E_p \approx E_p(t \approx \Delta)$, where Δ is approximately the peak time of the pulse. For α not very different from 1, integration of $d^2 N(E, t) / dE dt$ from $E = E_m$ upwards yields

$$(5) \quad N(t, E > E_m) \propto \frac{t^2}{(t^2 + \Delta^2)^2} \exp(-E_m / E_p(t)).$$

A best fit of Eq.(5) to the observed pulse shape (Goldstein et al. 2017) for $E_m = 50$ keV, which is shown in Figure 2, returns $\Delta = 0.54$ s, $\tau = 0.65$ s, and $E_p(0) = 260$ keV. The best fit value of Δ yields $E_p \approx E_p(\Delta) = 94$ keV, while $\tau = 0.65$ s yields a PWN radius $R \approx 1.3 \times 10^{15}$ cm.

3. – Extended emission

A considerable fraction of SHBs show an extended emission (EE) after the prompt SHB (Villasenor et al. 2005; Norris & Bonnell 2006; Fong & E. Berger 2013; Berger 2014

for a review). Such SHBs may take place in rich star clusters or globular clusters (GCs) (DDD 2009b), where the ratio of neutron stars to main sequence stars is much higher than in the regular interstellar medium of galaxies.

When the ICS of the ambient light in a GC by a CB launched in NSMs takes over the fast decay of the prompt emission, the CB is already transparent to radiation, and its EE light curve has a form similar to that of the decay phase of the prompt emission in Eq.(5),

$$(6) \quad E \frac{d^2 N_\gamma}{dE dt} \propto \frac{1}{(t^2 + \Delta'^2)} E^{1-\alpha'} \exp(-t/\tau'(E))$$

where primes indicate GC values, i.e., $\Delta' \approx (1+z) R_{GC}/\gamma \delta c$, and $\tau'(E) = \epsilon'_p R_{GC}/c E$.

The follow up observations of SHB170817A may have started too late for detection of an extended emission. However, if indeed SHB170817A did not take place in a GC or a bright location in its host galaxy NGC4993 (Levan et al. 2017), then no EE was expected in the CB model.

4. – The early afterglow

The X-ray afterglow of ordinary SHBs are well explained by PWN emission powered by the rotational energy loss through magnetic dipole radiation (MDR), relativistic winds and high energy particles of the nascent millisecond pulsars (MSPs) in NSMs (Dado & Dar 2017). In a steady state, the X-ray luminosity powered by the spin-down of the MSP has the form

$$(7) \quad L_b \approx L_{msp}(0) [1 - e^{-t^2/2t_r^2}] / (1 + t/t_b)^2$$

where $t_r^2 = 3 N_e \sigma_T / 8 \pi c v$ and $t_b = P_i / 2 \dot{P}_i$ and $P_i = P(t=0)$ is the initial period of the nascent n*. This afterglow takes over during the fast decay phase of the prompt emission in SHBs without extended emission, or during the extended emission phase in SHBs with extended emission, respectively, as demonstrated in Figure 3 (Dado & Dar 2017).

The observed UVOIR afterglow of SHB170817A in the first two weeks after burst can be well explained by a PWN emission powered by the rotational energy loss of the nascent millisecond pulsars (MSPs) in NSMs (Dado & Dar 2017), or by the expansion of an Arnett-type fireball (Arnett 1982) powered by several sources. Such sources include neutrino-anti neutrino annihilation outside the merging n*s (Goodman, Dar & Nussinov 1987), decay of radioactive elements within merger ejecta (macronova) (Li & Paczynski 1998) and by the radiation, high energy particles and relativistic winds emitted from the binary n*n* before the merger, or by a nascent n* after the merger.

If the remnant of the NSM is a black hole within a fireball/macronova, which expands with a constant velocity v , its late time light curve after t_d , the time it becomes transparent to radiation, is given (Dado et al. 2017) by

$$(8) \quad L_b \approx L(t_d) e^{-t^2/(2t_r^2)}.$$

In Figure 4 we compare the bolometric light curve of the UVOIR afterglow of SHB170817A during the first two weeks after burst with that predicted for a PWN powered by a nascent millisecond pulsar or a fireball surrounding a nascent black hole. A best fit of Eq.(7) to the bolometric light curve of SHB170817A reported by Drout et al. (2017) and shown in

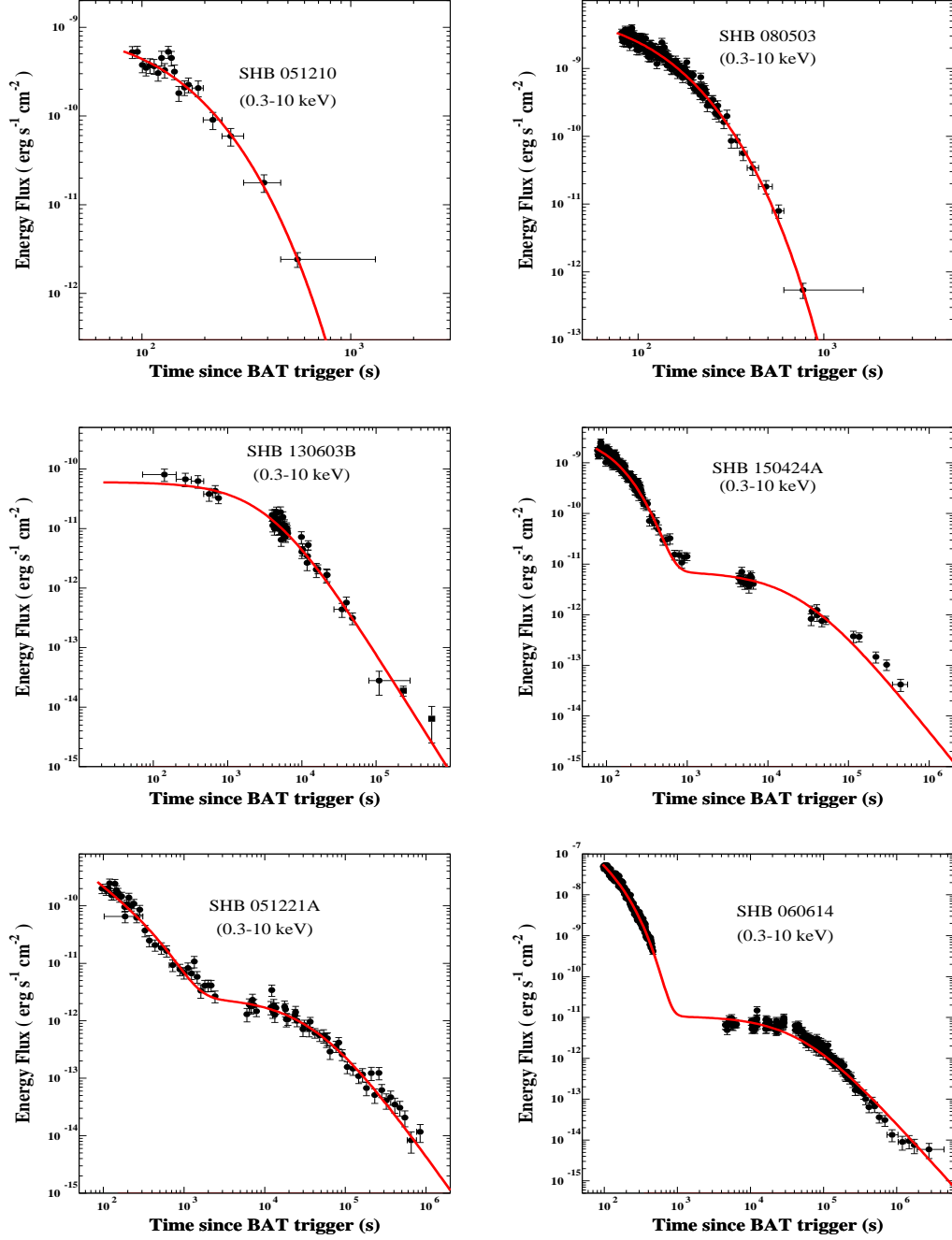


Fig. 3. – The X-ray light curves of a representative sample of SHBs with a well sampled X-ray afterglow observed before SHB170817A, and the best fits of ICS of glory light taken over by PWN emission powered by a millisecond pulsar (MSP).

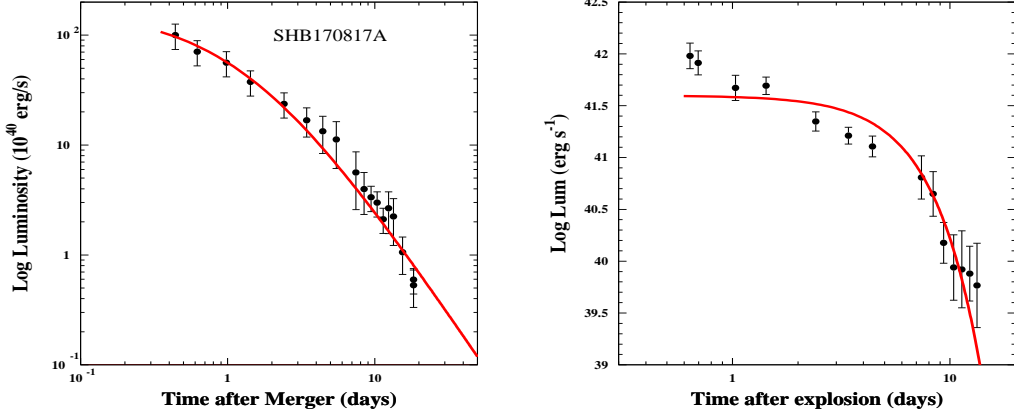


Fig. 4. – Left: The best fit CB model bolometric light curve of SHB170817A as give by Eq.(7) to that reported by Drout et al. (2017), assuming a neutron star remnant. Right: The best fit bolometric light curve of SHB170817A as given by Eq.(8) to that reported by Smartt et al. (2017), Evans et al. (2017), and Pian et al. (2017), assuming a black hole remnant.

Figure 4 yields $L_{msp}(0) = 2.27 \times 10^{42}$ erg/s, $t_b = 1.15$ d, and $t_r = 0.23$ d, with an entirely satisfactory $\chi^2/\text{dof} = 1.04$.

The CB model best fits to the measured bolometric light curves of the UVOIR afterglow of SHB170817A in the first two weeks after burst, as shown in Figure 4, suggest that the compact remnant of NSM170817 is a pulsar rather than a stellar mass black hole. Indeed, the UVOIR afterglow of SHB170817A observed at $t > 0.4$ day has a very similar shape to the X-ray afterglows of SHBs 051221A and 060614 observed in the same time interval, as shown in Figure 3.

5. – The far off-axis late-time afterglow

The circumburst medium in the path of a CB moving with a Lorentz factor $\gamma \gg 1$ is completely ionized by the CB’s radiation. The ions of the medium that the CB sweeps in generate within it turbulent magnetic fields. The electrons that enter the CB with a Lorentz factor $\gamma(t)$ in its rest frame are Fermi accelerated there, and cool by emission of synchrotron radiation, an isotropic afterglow in the CB’s rest frame. As for the rest of the CB’s radiations, the emitted photons are beamed into a narrow cone along the CB’s direction of motion, their arrival times are aberrated, and their energies boosted by the Doppler factor $\delta(t)$ and redshifted by the cosmic expansion.

The observed spectral energy density of the *unabsorbed* synchrotron afterglow has the form (e.g., Eq. (28) in DDD 2009a)

$$(9) \quad F_\nu \propto [\gamma(t)]^{3\beta-1} [\delta(t)]^{\beta+3} \nu^{-\beta},$$

where β is the spectral index of the emitted radiation at a frequency ν . The swept-in ionized material decelerates the CB’s motion. Energy-momentum conservation for such a plastic collision between a CB of baryon number N_B , radius R_{CB} , and an initial Lorentz

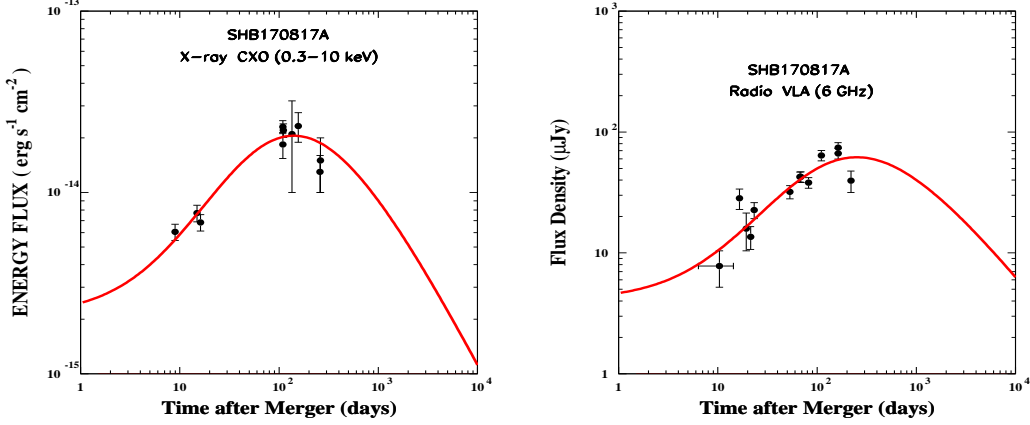


Fig. 5. – Left: Comparison between the light curve of the X-ray afterglow of SHB170817A measured with the CXO (Troja et al. 2017a,b; Margutti et al. 2017a,b; Haggard et al. 2017; Alexander et al. 2018) and the light curve expected in the CB model as described in the text. Right: Comparison between the 6 GHz light curve of the afterglow of SHB170817A measured with the VLA (Hallinan et al. 2017; Mooley et al. 2018; Margutti et al. 2018; Alexander et al. 2018) and the light curve expected in the CB model as described in the text.

factor $\gamma_0 \gg 1$ yields the deceleration law (e.g. Eq. (3) in Dado & Dar 2012)

$$(10) \quad \gamma(t) = \frac{\gamma_0}{[\sqrt{(1+\theta^2 \gamma_0^2)^2 + t/t_s} - \theta^2 \gamma_0^2]^{1/2}},$$

where $t_s = (1+z) N_B / (8 c n \pi R_{CB}^2 \gamma_0^3)$ is the slow-down time scale. The frequency and time dependence of the afterglow that follow from Eqs. (9),(10) depend only on three parameters: the product $\gamma_0 \theta$, the spectral index β , and the slow-down time-scale t_s . For $t \gg t_b = (1+\theta^2 \gamma_0^2)^2 t_s$, Eq. (10) yields $\gamma(t) \propto t^{-1/4}$, and consequently a power-law decline, $F_\nu(t) \propto t^{-(\beta+1/2)} \nu^{-\beta}$, independent of the values of t_b and $\gamma(0) \theta$. In Figure 5 we compare the observed light curves of the late-time radio and X-ray unabsorbed afterglows of SHB170817A and those predicted by Eq.(9), for the observed 0radio to X-ray spectral index $\beta = 0.57 \pm 0.09$, Eq. (10) for $\gamma(t)$ with $\gamma(0) \theta = 5$ estimated from the measured $E_p = 82$ keV, and $t_s = 0.137$ days obtained from a best fit to the X-ray data.

6. – Superluminal motion

A very specific prediction of the CB model is an apparent superluminal speed V_{app} in the plane of the sky, relative to launch sites (Dar & De Rujula 2000b; DDD 2016 and references therein), of the CBs moving towards the observer at a small but not vanishing angle θ , which satisfies

$$(11) \quad V_{app} \approx [2 \gamma(t)^2 \theta / (1 + \theta^2 \gamma(t)^2)] c$$

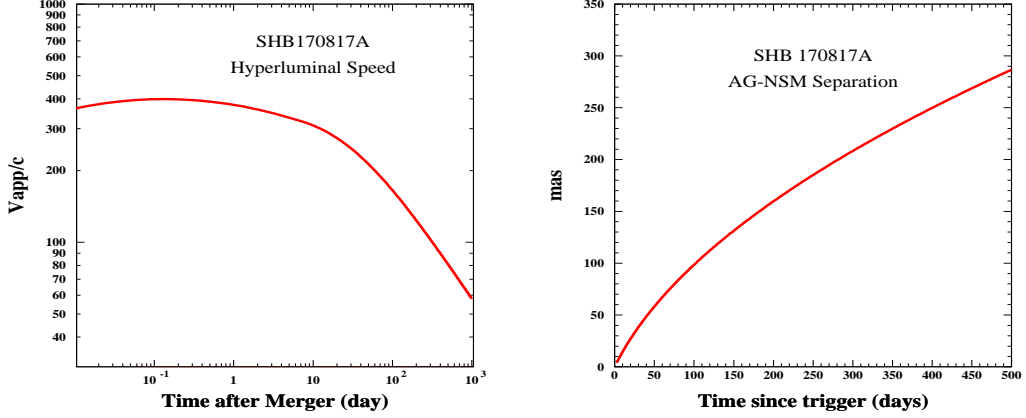


Fig. 6. – CB model estimate of the superluminal speed (left) and angular displacement (right) of the leading CB relative to the location of SHB170817A as a function of time after burst.

with $\gamma(t)$ as in Eq.(10). The angular displacement $\alpha(t)$ from the location of the neutron star merger to the CB's later position is:

$$(12) \quad \alpha(t) = c \int_0^t dt' V_{app}(t') / D_A ,$$

where D_A is the angular distance to the SHB. In Figure 6 we plot the estimated superluminal speed and angular displacement expected for SHB170817A in the CB model, for $\gamma(0) \approx 10^3$ $\theta \approx 5$ mrad $t_s = 0.167$ d, and $D_A = 39.6$ Mpc the angular distance to SHB170817A in the standard cosmology.

7. – Conclusions

1. The temporal and spatial coincidence of GW170817 and SHB170817A has shown beyond doubt that n*n* mergers produce SHBs.

2. The observed properties of SHB170817A, that appear different from those of ordinary SHBs, are those expected in the CB model for an ordinary SHB viewed from far off-axis.

3. In spite of the CB-model's simplicity, it reproduces very well the γ -ray pulse, the following UVOIR emission and the light curves of the late-time radio to X-ray afterglow of SHB170817A. The underlying model intrinsic and environmental parameters extracted from both the pulse and the afterglow are very consistent. Moreover, they are compatible with our previous CB model analysis of GRB and SHB pulses and afterglows. They suggest that:

4. The n*n* binary was produced in a common envelope core collapse SN.

3. The remnant of NSM170817 was a neutron star and not a black hole.
4. The n^*n^* merger took place inside a PWN.
5. The observed UVOIR light from SHB170817A in the first 2 weeks after burst, probably, was that of PWN powered by the nascent MSP.
6. The late-time radio to X-ray afterglow is the synchrotron radiation expected from the deceleration in the ISM of a highly relativistic jet viewed from far off-axis.
7. The radio AG of SHB170817A still provides a rare opportunity to observe an apparent superluminal jet.
8. SHB170817A does not provide compelling evidence that GW170817 produced kilonova.
10. The smoking guns of Ligo-Virgo detected n^*n^* mergers will only be far off-axis SHBs or orphan afterglows.

Acknowledgment: We are grateful to A. De Rújula for a long and fruitful collaboration in the development of the CB model and its many applications.

References:

- Abbott, B.P., et al. [Ligo-Virgo Collab.] 2017a, PRL, 119, 161101 [arXiv:1710.05832]
 Abbott, B.P., et al. [Ligo-Virgo-Fermi-Integral Collab.] 2017b, ApJ, 848, L12 [arXiv:1710.05834]
 Abbott, B.P. et al., [Ligo-Virgo Collab.], 2017c, ApJ, 851, L16 [arXiv:1710.09320]
 Alexander, K.D., Margutti, R., Blanchard, P.K., et al. 2018 [arXiv:1805.02870]
 Amati, F., Frontera, M., Tavani, J.J.M., et al., 2002, A&A, 390, 81A [astro-ph/0205230]
 Arnett, W.D., 1982, ApJ, 253, 785A
 Badde, W. & Zwicky, F., 1934, PRL 46(1), 76
 Bell, S.J. & Hewish, A., 1967, Nature 213, 1214.
 Berger, E., 2014 ARA&A, 52, 43 [arXiv:1311.2603]
 Berger, E., Fong, W., Chornock, R. 2013, ApJ, 774, L23 [arXiv:1306.3960]
 Bhattacharya, D. & van den Heuvel, E.P.J., 1991, PhR, 203, 1124.
 Chamel, N. & P. Haensel, P., 2008, Living Rev. Rel. 11, 10 [arXiv:0812.3955]
 Costa, E., Frontera, F., Heise, J., et al. 1997, Nature, 387, 783 [astro-ph/9706065]
 2017, ApJ, 848, 17 [arXiv:1710.05840]
 Dado, S. & Dar, A., 2012, ApJ. 761, 148 [arXiv:1203.1228]
 Dado, S. & Dar, A., 2016, PhRvD, 94, 300 [arXiv:1603.06537]
 Dado, S. & Dar, A., 2017, arXiv:1708.04603
 Dado, S., Dar, A., De Rújula, A., 2002, A&A, 388, 1079 [arXiv:astro-ph/0107367]
 Dado, S., Dar, A., De Rújula, A., 2009a, ApJ, 696, 994 [arXiv:0809.4776]
 Dado, S., Dar, A., De Rújula, A., 2009b, ApJ, 693, 311 [arXiv:0807.1962]
 Dado, S., Dar, A., De Rújula, A., 2016 [arXiv:1610.01985]
 Dado, S., Dar, A., De Rújula, A., 2017 [arXiv:1712.09970]
 Dar, A. & De Rújula, A., 2000a [arXiv:astro-ph/0008474]
 Dar, A. & De Rújula, A., 2000b [arXiv:astro-ph/0012227]
 Dar, A. & De Rújula, A., 2004, PhR, 405, 203 [arXiv:astro-ph/0308248]
 Dar, A., Kozlovsky, Ben Z., Nussinov, S., Ramaty, R., 1992, ApJ, 388, 164

- Drout, M.R., Piro, A.L., Shappee, O.B.J. et al. 2017, *Sci.* 358, 1570 [arXiv:1710.054431]
 Evans, P.A., Cenko, S.B., Kennea, J.K., et al. 2017, *Sci.* 358, 1565 [arXiv:1710.05437]
 Fong, W. & Berger, E., 2013, *ApJ*, 776, 18 [arXiv:1307.0819]
 Gaensler, B. & Slane, P.O., 2006, *ARAA*, 44, 17
 Galama, T.J., et al. 1998, *Nature* 395, 670 [astro-ph/9806175]
 Goldstein, A. Veres, P., Burns, E., et al. 2017, *ApJ*, 848, L14 [arXiv:1710.05446]
 Goodman, J., 1986, *ApJ*, 308, L47
 Goodman, J., Dar, A., Nussinov, S. 1987, *ApJ*, 314, L7 (1987)
 Haggard, D., John, J., Ruan, J.J., et al. 2017, *GCN* 22206
 Hallinan, G., Corsi, A., Mooley, K.P., et al. 2017, *Sci.* 358, 1559 [arXiv:1710.05435]
 Hjorth, J., et al. 2003, *Nature*, 423, 847 [astro-ph/0306347]
 Hulse, R.A. & Taylor, J.H., 1975, *ApJ*, 195, L51
 Hewish, A., et al. 1968, *Nature*, 217, 709.
 Klebesadel, R.W., Strong, I.B. & Olson R.A., 1973, *ApJ*, 182, L85
 Kouveliotou, C., et al. 1993, *ApJ*, 413, L101
 Levan, A.J., Lyman, J. D., Tanvir, N.R., et al. 2017, *ApJ*, 848, L28 [arXiv:1710.05444]
 Li, L.X., & Paczynski, B., 1998, *ApJ*, 507, L59 [astro-ph/9807272]
 Lorimer, D.R., 2008 *Living Rev. Relativity*, 11, 8 [arXiv:0811.0762]
 Macias-Perez, J.F., Mayet, F., Aumont, J., Dert, F. X., 2010, *ApJ*, 711, 417 [arXiv:0802.0412]
 Margutti, R., Berger, E., Fong, W., et al. 2017a, *ApJ*, 848, L20 [arXiv:1710.05431]
 Margutti, R., Fong, W., Eftekhari, T., et al. 2017b, *GCN* 22203
 Margutti, R., Alexander, K.D., Xie, X., et al, 2018, *ApJ*, 856, L18 [arXiv:1801.03531]
 Meegan, C.A., Fishman, G.J., Wilson, R.B., et al. 1992, *Nature*, 355, 143
 Meszaros, P., 2001, *PThPS*, 143, 33
 Mooley, K.P., Nakar, E., Hotokezaka, K., et al. 2018, *Nature*, 554, 207 [arXiv:1711.11573]
 Norris, J.P. & Bonnell, J.T., 2006, *ApJ*, 643, 266 [arXiv:astro-ph/0601190]
 Norris, J.P., Cline, T.L., Desai, U.D., Teegarden, B.J., 1984, *Nature*, 308, 434
 Pacini, F., 1967, *Nature*, 216, 567
 Pian, E., D’Avanzo, P.S. Benetti, S., et al. 2017, *Nature*, 551, 67 [arXiv:1710.05858]
 Piran, T., 1999, *PhR*, 314, 575 [arXiv:astro-ph/9810256]
 Savchenko, V., Ferrigno, C., Kuulkers, E., et al. 2017, *ApJL*, 848, L15 [arXiv:1710.05449]
 Shviv, N. & Dar, A., 1995, *ApJ*, 447, 863 [arXiv:astro-ph/9407039]
 Smartt, S.J., Chen, T.W., Jerkstrand, A., et al. 2017, *Nature*, 551, 75 [arXiv:1710.05841]
 Stanek, K. Z., et al. 2003, *ApJ*, 591, L17 [arXiv:astro-ph/0304173]
 Tanaka, S. J., & Takahara, F., 2010, *ApJ*, 715, 1248 [arXiv:1001.2360]
 Taylor, J.H. & Weisberg, J.M., 1984, *PRL*, 52, 1348
 Taylor, J.H. & Weisberg, J.M., 1989, *ApJ*. 345, 434
 Troja, E., Piro, L., van Eerten, H., et al. 2017a, *Nature*, 551, 71 [arXiv:1710.05433]
 Troja, E., Piro, L., van Eerten, H., et al. 2017b, *GCN* 22201 (2017)
 Villasenor, J.S., Lamb, D.Q., Ricker, G.R., et al. 2005, *Nature*, 437, 85 [astro-ph/0510190]
 von Kienlin, A., Meegan, C., Goldstein, et al. 2017, *GCN Circular* 21520
 Wagoner, R.V., 1975, *ApJ*, 196, L63
 Weiler, K.W. & Panagia, N., 1978, *A&A*, 70, 419
 Zeh, A., Klose, S., Hartmann, D.H., 2004, *ApJ*, 609, 952 [astro-ph/0311610]